IEEE Photonics Journal
An IEEE Photonics Society Publication

Open Access

Study on the Key Technology of Image Transmission Mechanism Based on Channel Coding Ghost Imaging

Volume 10, Number 4, August 2018

Leihong Zhang
Ye Hualong
Dawei Zhang

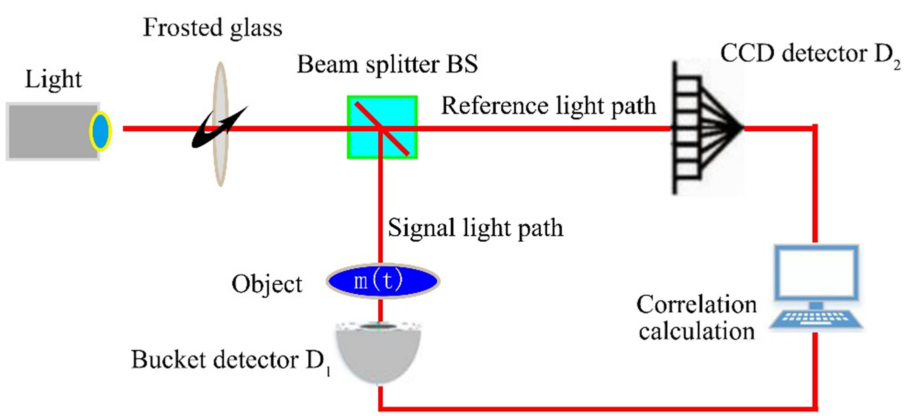

DOI: 10.1109/JPHOT.2018.2858823
1943-0655 © 2018 IEEE

Study on the Key Technology of Image Transmission Mechanism Based on Channel Coding Ghost Imaging

Leihong Zhang,[1] **Ye Hualong**,[1] **and Dawei Zhang**[2]

[1]College of Communication and Art Design, University of Shanghai for Science and Technology, Yangpu Qu 200093, China
[2]School of Optical Electrical and Computer Engineering, University of Shanghai for Science and Technology, Yangpu Qu 200093, China

DOI:10.1109/JPHOT.2018.2858823
1943-0655 © 2018 IEEE. Translations and content mining are permitted for academic research only. Personal use is also permitted, but republication/redistribution requires IEEE permission. See http://www.ieee.org/publications_standards/publications/rights/index.html for more information.

Manuscript received May 26, 2018; revised July 17, 2018; accepted July 19, 2018. Date of publication July 26, 2018; date of current version August 1, 2018. This work was supported in part by Natural Science Foundation of Shanghai under Grants 4ZR1428400 and 18ZR1425800, and in part by Open Project of Anhui Province Key Laboratory of Nondestructive Evaluation under Grant CGHBMWSJC03.
Corresponding author: Ye Hualong (e-mail: yehualong930912@sina.com).

Abstract: Based on the analysis of the algorithm of ghost imaging and channel coding transmission, this paper combines the error detection and correction function of channel coding and accurate transmission of ghost imaging to complete image coding transmission. The mechanism of image transmission based on channel coding ghost imaging is studied. Compared with the traditional algorithm of ghost imaging, the mechanism of image coding and transmission greatly decreasing the error rate, reducing the storage space, enhancing the ability of anti-jamming and anti-interception, and realizing the accurate image coding transmission. It solves problems such as insufficient feasibility, low reduction degree, long imaging time of current imaging algorithm, and so on.

Index Terms: Channel coding, error correction matrix, ghost imaging, image transmission.

1. Introduction

In the field of image transmission, it is often necessary to transfer images from one processing unit to another. In the transmission process, the data of image signal and effective signal is first encoded, then transmitted to another processing unit and decoded [1]. Ghost imaging is a new high resolution imaging technology and has developed in recent years [2]–[10]. Klyshko proposed the scheme of ghost imaging based on the entanglement behavior of the converted photon pairs with spontaneous parameters [11]. Shapiro and Bromber [12] used spatial light modulator (SLM) to preset the illuminating speckle field of the object to realize the computational ghost imaging. Zhong Y J [13] proposed a new ghost imaging scheme with multiple speckle patterns and applied ghost imaging to image transmission. In the digital transmission system, the transmission channel inevitably has certain interference, the information produces the error in the transmission process. In order to correct errors and ensure communication quality, channel coding [14] technology has been rapidly developed. The technology is used to transmit information and resist various kinds of interference during transmission. In reference [15], a kind of secure communication method based on Low Denglty Parlty Check (LDPC) codes is proposed, which is based on the symmetric cryptography of error-correcting codes and the performance equivalent coding matrix. Without changing

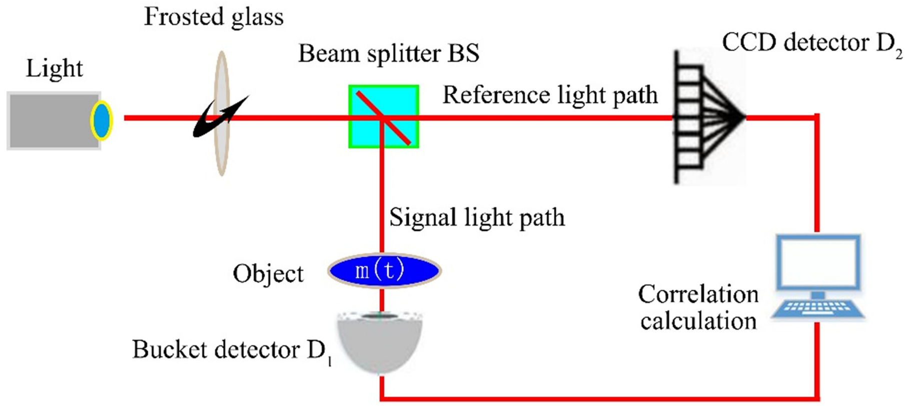

Fig. 1. Principle of ghost imaging.

the error-correcting capability, it increased the difficulty for non-partners to identify the cracked information. In reference [16], a simple and efficient method for generating the observation matrix is proposed, and LDPC mechanism is also introduced. In reference [17], it is proposed to improve the efficiency of image coding transmission by optimizing the extraction and reconstruction of image transmission. In reference [18], the adaptive transformation of the Discrete Cosine Transform (DCT) is proposed, which is based on the application of image coding and makes effective use of the statistical characteristics of the image. In reference [19], a surface-to-point optical wireless communication mechanism is proposed, which improves the optical wireless communication capability in a chaotic and turbulent atmosphere. At present, optical communication image transmission mainly uses the point-to-point transmission mode. This transmission mode has poor anti-interference ability, high bit error rate, poor image reconstruction quality, and low transmission efficiency of the image. In this paper, the mechanism of ghost imaging based on channel coding is studied. The main purpose is to reduce the bit error rate in information transmission as much as possible, in the most effective use of the channel transmission capacity. The algorithm of ghost imaging is used to improve the reliability of transmission signal and ensure the quality of data transmission.

2. Computational Ghost Imaging

Ghost imaging is a new imaging method, which uses quantum entanglement to image. The object information is obtained by a high-order correlation using two detectors to measure the light intensity distribution of two light paths. The principle is shown in Fig. 1.

Ghost imaging experiments first use a two-photon entangled light source, and then proves that the classical pseudo-thermal light field can also achieve ghost imaging through theoretical derivation and experimental simulation. The presetting optical field is used to calculate ghost imaging, which saves the free optical path of detecting the distribution of optical field. Computational ghost imaging not only inherits the important characteristics of ghost imaging in terms of imaging principle, but also makes the optical system more simple in structure, stronger ability to resist external interference and better imaging effect. As shown in Fig. 2, a barrel detector with no spatial resolution is used to collect the light intensity values of the diffracted object. Since there are only one probe path and one barrel detector, the imaging does not depend on the non-local entangled two-photon interference. An important device in the experiment is the liquid crystal spatial Light modulator (SLM), which is placed on the arm of the detecting optical path. By controlling the beam to hit the object to be imaged, these beams are transmitted to the spatial light modulator and reflected by a series of phase random pictures, which are time-independent from each other. The barrel-detector is placed at the end and the total light intensity is collected after the object is diffracted.

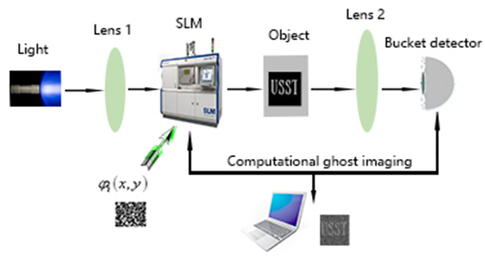

Fig. 2. Schematic diagram of computational ghost imaging.

$\varphi_i(x,\ y)$ obeys the uniform distribution on $[0, 2\pi]$. Spatially correlated monochromatic laser light irradiates vertically the SLM of the spatial light modulator. The SLM only modulates the phase of the light based on the input phase picture. The light field distribution is $\{I_i(x,\ y)\}$. The random spot generated is irradiated on the object T(x, y) to be imaged after the SLM, and the intensity of light diffracted by the object is collected by bucket detector to calculate the light intensity value B_i.

According to the Fresnel propagation function, the formula is as follows:

$$B_i = \int dxdy\ I_i\,(x, y) \times T\,(x, y) \tag{1}$$

$$I_i\ \ (x, y) = |E_{in}\,(x, y)\,exp\,[j\varphi_i\,(x, y)] \otimes h_z\,(x, y)| \tag{2}$$

$h_z(x,\ y)$ is the Fresnel diffraction function for a distance z, and $\otimes$ stands for convolution. Then use the ghost function to restore the original information of the object. The expression of the procedure is as follows:

$$T_{GI}\ \ (x, y) = \frac{1}{N}\sum_{i=1}^{N}(B_i - B)\,I_i\,(x, y) \tag{3}$$

In the formula (3), B represents the average light intensity.

In this paper, the combination of channel coding and the algorithm of ghost imaging greatly simplifies the computational workload. At the same time, the imaging quality can be improved under the same calculation conditions. For the transmission of images, the pixel points are composed of different values, so it is easy to produce errors in the transmission process. The binary coding is introduced to realize the different images with 0 and 1. While the transmission is accurate, the threshold value is also introduced to achieve accurate reconstruction and complete image coding transmission.

3. Channel Coding

Channel coding is an important communication error correction method. The principle of error correction coding is added to the ghost imaging to improve the channel decoding performance of visible light communication, raise the efficiency of information transmission and reduce the decoding complexity. Nowadays, LDPC codes have become an integral part of optical communication systems and are used to detect and correct information transmission errors caused by channel effects. Robert Gallager first discussed error correction codes based on the LDPC (Low Denglty Parlty Check) code in his doctoral dissertation [20]. Compared with other codes, LDPC codes have the best performance, and the decoding complexity of LDPC codes is much smaller. The verification matrix of LDPC code is flexible in construction and simple in expression, and the verification matrix can be verified according to relevant theories; the low density of LDPC codes results in low decoding complexity, and the decoding method can be implemented in parallel operations; the low density and parity of the LDPC codes make it relatively easy to implement in hardware, and has high throughput decoding potential.

For a block code of length n, the information symbol is k bits, and the supervision symbol is $r = n - k$ bits (generally denoted as (n, k) code). If r supervised bits are used to construct r supervised relations to indicate n possible cases of an error code, then there are requirements: $2^r - 1 \geq n$ or $2^r \geq k + r + 1$. Let k = 4 among the block codes (n, k), in order to be able to correct one bit error, it is required to satisfy $r \geq 3$ and let $r = 3$, then $n = k + r = 7$. The constraints of the (7, 4) linear block code supervising bits and information bits are as follows:

$$\begin{aligned} c5 &= c1 + c2 + c3 \\ c6 &= c2 + c3 + c4 \\ c7 &= c1 + c2 + c4, \end{aligned}$$

according to the constraint relation, the generation matrix G can be obtained:

$$G = [I_K Q] = \begin{bmatrix} 1\,0\,0\,0\,1\,0\,1 \\ 0\,1\,0\,0\,1\,1\,1 \\ 0\,0\,1\,0\,1\,1\,0 \\ 0\,0\,0\,1\,0\,1\,1 \end{bmatrix},$$

then the entire code group can be generated: A = CG, A is the symbol after encoding, and C is the information symbol at the sending end. From the relationship between the generator matrix and the check matrix: $GH^T = 0$, finally, the check matrix can be obtained:

$$H = \begin{bmatrix} 1\,1\,1\,0\,1\,0\,0 \\ 0\,1\,1\,1\,0\,1\,0 \\ 1\,1\,0\,1\,0\,0\,1 \end{bmatrix}.$$

If the received code word is R, then the concomitant $S = RH^T$. can be defined. S is also called the syndrome. Let $S' = S \, mod 2$, and let each column of H be added to S'. in sequence. If the sum is a zero matrix, it means that there is an error in the ith code word in the received R, which must be corrected.

4. Image Transmission Mechanism Based on Channel Coding Ghost Imaging

The information transmission process based on the algorithm of channel coding ghost imaging in this paper is shown in Fig. 3. Research achieves accurate image encoding transmission through correlated imaging.

Here, the pixels that transmit the signal image are represented by different values. In order to ensure the precision and robustness in the transmission process, the values of different sizes are converted into binary, and different images are represented by 0 and 1 code. The encoded image is transmitted to the receiver through the optical fiber, and the receiver uses the barrel detector to receive the transmitted information. After the encoded information is transmitted multiple times, the transmission process is completed. The basic process is as follows:

1) According to the error correction principle of the (7, 4) linear block code, the N*N image is first linearly coded, and the N*N pixels of the two-dimensional image are converted into a one-dimensional sequence ($1*N^2$ pixel);
2) Every four codewords are grouped into a group and linearly coded according to the principle of (7, 4) linear block code, and the data after coding is correlated and imaged;
3) Since some values become decimals in the simulation process and are no longer 0 and 1, therefore, a threshold is set to judge, and the data of encoded and correlated imaged are obtained;
4) One-dimensional sequence is obtained after error correction decoding, then converted into a two-dimensional sequence, and finally the original image can be recovered.

Taking C = [1 1 0 0] is the information code word to be encoded, which becomes A = [1 1 0 0 0 1 0] after the encoding. If the code word is R = [0 1 0 0 0 1 0] received through ghost

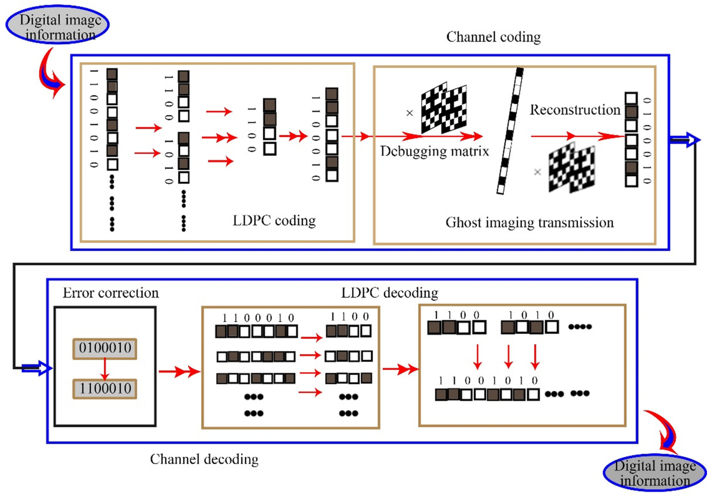

Fig. 3. Information transmission process based on the algorithm of channel coding ghost imaging.

imaging and threshold judgment, and then $S' = [1\ 0\ 1]$ can be obtained by calculation,

$$H' = \begin{bmatrix} 0\ 0\ 0\ 1\ 0\ 1\ 1 \\ 0\ 1\ 1\ 1\ 0\ 1\ 0 \\ 0\ 0\ 1\ 0\ 1\ 1\ 0 \end{bmatrix},$$

we can see that the first column is zero matrix, indicating that the first code word is wrong. After correction, it becomes $R' = [1\ 1\ 0\ 0\ 0\ 1\ 0]$, which is the original code word. The (7, 4) linear block code used here is a kind of LDPC code. The main encoding methods of LDPC codes at present are the Gaussian elimination method, approximate triangles method, and special code words method. The Gaussian elimination method is used here. Gaussian elimination does not lose performance when it is transformed.

5. Simulation and Result Analysis

5.1 Simulation

According to the principle of (7, 4) linear block code, the two-dimensional pixel matrix of the USST map is converted into a one-dimensional vector for group coding, after ghost imaging, error detection and error correction decoding is performed, and finally the original image is recovered. In the process of simulation experiments, a picture of size $64 * 64$ is firstly selected. According to the error correction principle of (7, 4) linear block code encoding and decoding, the $64 * 64$ size picture is linearly encoded, and the $64 * 64$ pixels in the image are converted into a one-dimensional sequence, that is $1 * 4096$ pixels, and then every four codewords are grouped into a set of linear coding according to the principle of (7, 4) linear block code, and the data is performed ghost imaging after coding. The threshold is set to 0.5 according to the algorithm principle of the ghost imaging. After judgment, the data output greater than 0.5 is 1, otherwise the output is 0. The output codeword is checked for error correction to detect the error code bit, and then the error correction decoding is performed to obtain a one-dimensional sequence, which is then converted into a two-dimensional sequence. Finally, the effect image can be restored, the effect image and the original image are analyzed and compared. Through the study of the ghost imaging mechanism based on channel coding, this paper uses MATLAB R2014b software simulation to achieve. The effect images produced by the two different methods are compared, which are obtained from traditional ghost imaging and channel-based ghost imaging of the original image. The simulation results are

TABLE 1
Effect Under Different Sampling Time

Sampling Ratio	15%	35%	55%	75%	95%
Ghost imaging					
Channel coding + Ghost imaging					

TABLE 2
Bit Error Rate

Sample times	Ghost imaging	Channel coding + Ghost imaging
896	0.2856	0.2751
1696	0.2368	0.2302
2496	0.1897	0.1780
3296	0.1379	0.1296
4096	0.1040	0.0900

TABLE 3
Information Entropy Comparison Table of the Two Samples With Different Sampling Times

	896	1696	2496	3296	4096
Ghost imaging	0.3899	0.3855	0.3633	0.3534	0.3433
Channel coding + Ghost imaging	0.3989	0.3738	0.3233	0.2824	0.2334

shown in Table 1 below. From the simulation results, it can be seen that the effect image obtained by the latter come closer to the original image.

5.2 Result Analysis

By combining the channel coding technique with the ghost imaging, the problem of reducing the detail of the object and the imaging time are further solved. This paper combines the channel

TABLE 4
Simulation Comparison Under Different Salt-Pepper Noises

sample times	96	896	1696	2496	3296	4096
Salt& Pepper 0.01		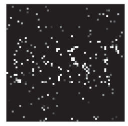				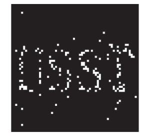
Salt& Pepper 0.02		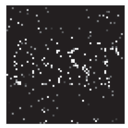	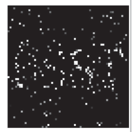			
Salt& Pepper 0.04						

TABLE 5
Simulation Comparison Under Different Speckle Noises

sample times	96	896	1696	2496	3296	4096
Speckle 0.1						
Speckle 0.2	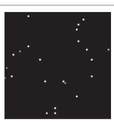	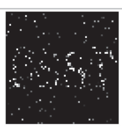	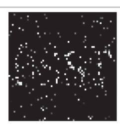			
Speckle 0.4		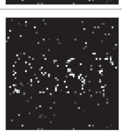	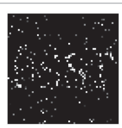		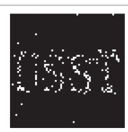	

coding technique and the ghost imaging, and proposes the algorithm of ghost imaging based on channel coding. Through the study of the ghost imaging mechanism based on channel coding, this paper uses MATLAB R2014b software simulation to achieve. The selected experimental object size is a 64×64 binary image (USST). Experimental simulation is analyzed and verified in terms of feasibility, bit error rate, reliability and robustness.

5.2.1 Feasibility: Feasibility refers to the situation where the original picture and text information are restored by combining the channel coding with the ghost imaging. The algorithm feasibility of ghost imaging based on channel coding is analyzed here mainly through variance and correlation coefficients. The variance D(X) characterizes the dispersed degree of the random variable. Correlation coefficient is the quantity of linear correlation among research variables, which is a statistical

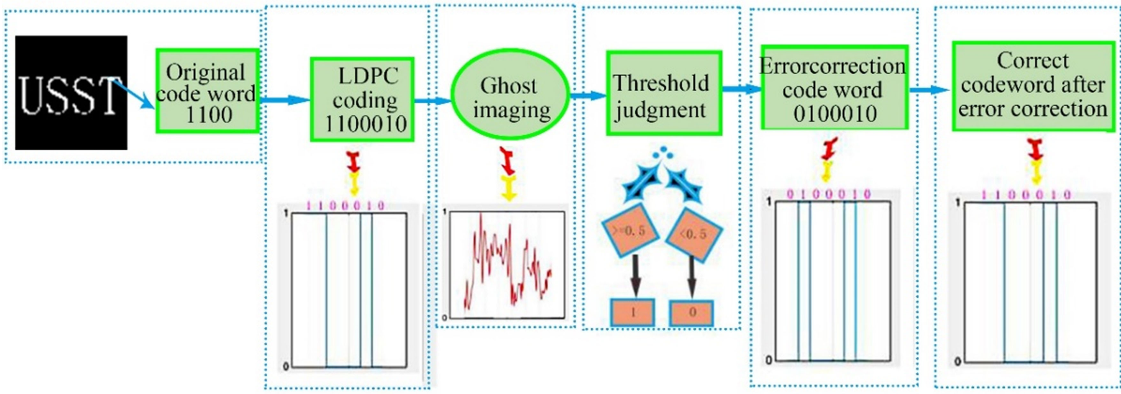

Fig. 4. Image data information transmission process.

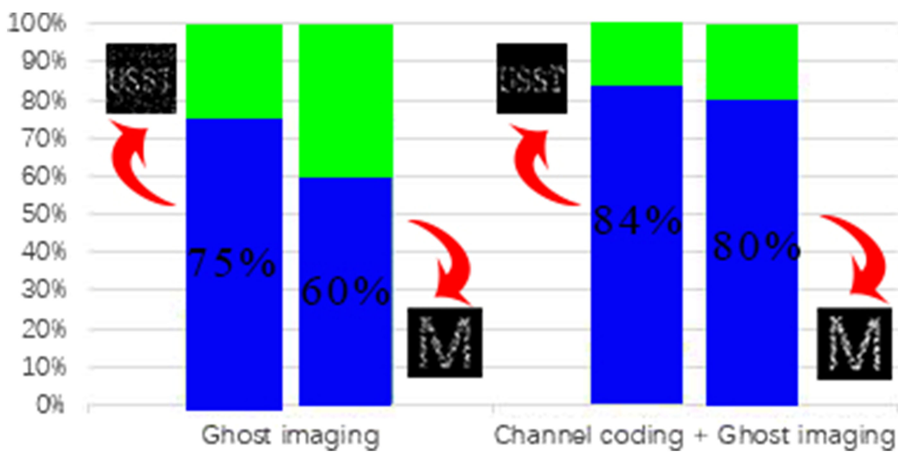

Fig. 5. Coefficients comparison of two different methods.

index to reflect the close relationship between variables.

$$\begin{cases} E\ (x) = \frac{1}{N}\ \sum_{i=1}^{N} x_i \\ D\ (x) = \frac{1}{N}\ \sum_{i=1}^{N} (x_i - E\ (x))^2 \\ cov\ (x, y) = \frac{1}{N}\ \sum_{i=1}^{N} (x_i - E\ (x))(y_i - E\ (y)) \\ CC = \frac{cov(x,y)}{\sqrt{D\,(x)}\sqrt{D\,(y)}} \end{cases} \tag{4}$$

Here, the correlation coefficient is represented by CC. The CC value is the larger, the degree of correlation is the greater, and the effect image clarity is the better, the feasibility of the scheme is the better. In pixel correlation coefficient calculation expression, x and y represent the pixel values of two adjacent pixels in the image, and CC is the correlation coefficient of two adjacent pixels.

From the bar graph in Fig. 5: (1) Since binary image is adopted in the simulation, the correlation coefficient is only 0 and 1, where green represents correlation coefficient 0, blue represents correlation coefficient 1. (2) As can be seen clearly in the figure, the proportion of the correlation coefficient of 1 is large, and the proportion of 0 is small, indicating that the image resolution of the effect is good. (3) For "USST," the algorithm of ghost imaging based on channel coding under the effect of image correlation coefficient of 1 to 84%, while the traditional algorithm of ghost imaging under the effect of image correlation coefficient is 1 only 75%, the former effect is better. For "M," the

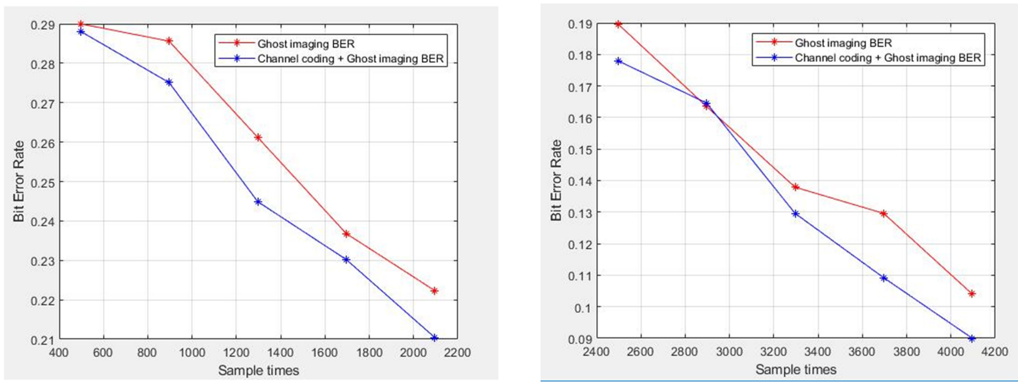

(a) (b)

Fig. 6. BER experimental value curve under different methods (a) BER value curve at low sampling times (b) BER value curve at high sampling times.

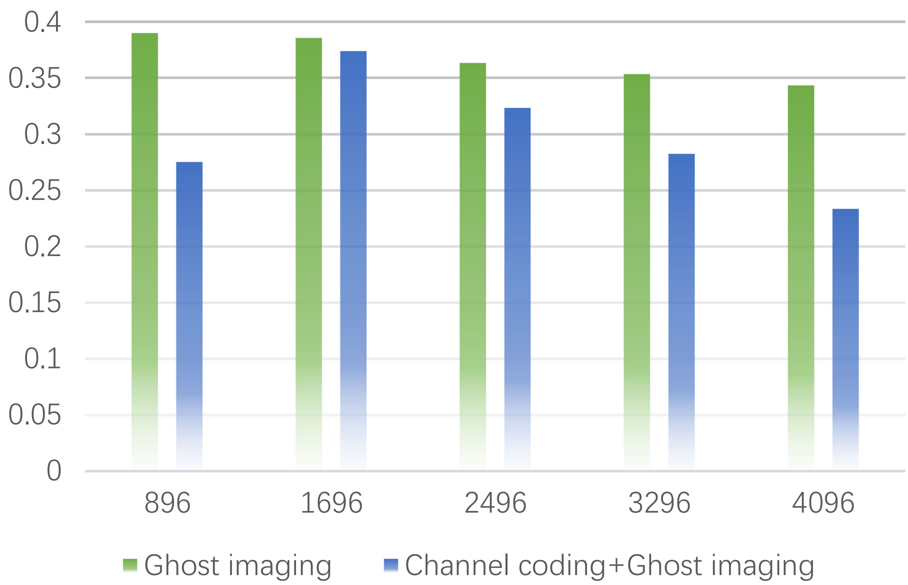

Fig. 7. The information entropy broken line graph of the two at different sampling times.

algorithm of ghost imaging based on channel coding under the effect of image correlation coefficient of 1 to 80%, while the traditional algorithm of ghost imaging under the effect of image correlation coefficient is 1 only 60%, the former effect is better in the same way. As the resolution of the effect image is proportional to the correlation coefficient, and the resolution of the effect image of this scheme is higher, it proves that this scheme is more effective in the feasibility evaluation index.

5.2.2 Bit Error Rate: For various reasons, digital signals inevitably generate errors during transmission. Due to the signal change in the signal transmission, the decay causes the corruption of signal and bit errors. Noise, pulses from alternating current or lightning, failure of transmission equipment, and other factors can cause bit errors (if the transmitted signal is 1, and received is 0; vice versa). If there is a bit error, there is a bit error rate. The BER: bit error rate is an indicator of the accuracy of data transmission over a specified period of time. Here the bit error rate is as an important indicator to measure the quality of the imaging algorithm.

In Fig. 6, the red color line represents the transformation of the BER value of the effect image under different sampling conditions in the conventional ghost imaging method, and the blue color

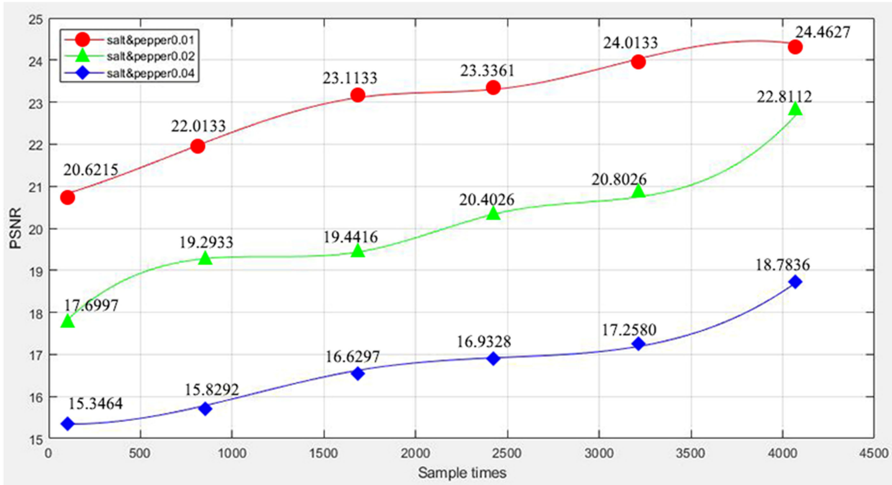

Fig. 8. PSNR values under different sampling times and salt-pepper noises.

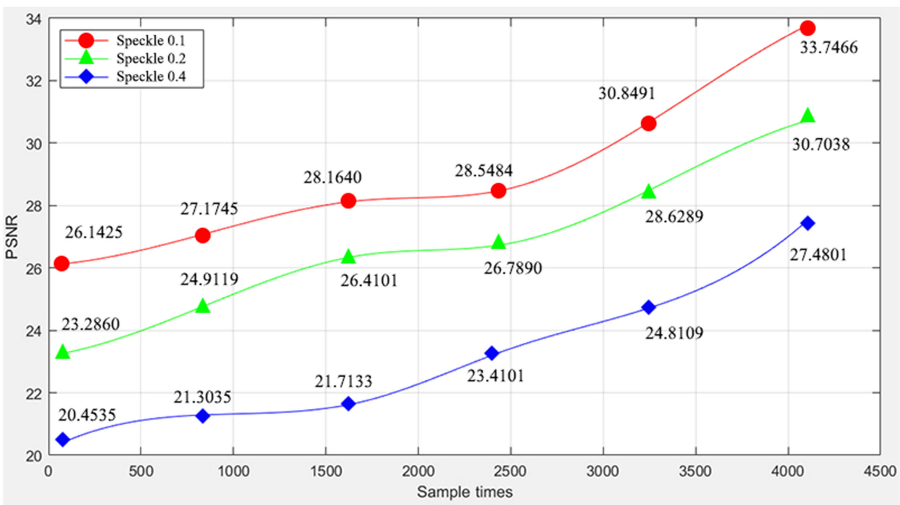

Fig. 9. PSNR values under different sampling times and speckle noises.

line represents the transformation of the BER value of the effect image under different sampling conditions with the algorithm of channel coding ghost imaging. The trend of line changes in the graph can be known as follows: (1) The BER value of the effect of the ghost imaging algorithm based on channel coding image is generally lower than the BER value of the traditional ghost imaging algorithm. The quality of the effect image is better, and it is closer to the original image information. (2) With the increasing of sampling times, the bit error rate gradually decreases, and when the sampling times are more than 4000, the BER value of the ghost imaging algorithm based on channel coding reaches 0.09, and the effect image is closer to the original image. However, the BER value of traditional ghost imaging algorithm is 0.1040, and the effect image is inferior to the former. (3) Under the lower sampling frequency, the BER of both values are very big and very close to, but with the increase of sampling frequency, the BER value gap increases gradually, when achieve high sampling frequency, the BER value of the gap is bigger, the effect the quality of the images also have obvious differences. These experimental results show that the effect image of this scheme has better quality, which proves that this scheme is more effective in measuring the error rate index.

5.2.3 Reliability: In order to objectively evaluate the quality of renderings and better describe the uncertainty of the system, the information entropy is used to analyze it. The concept of information entropy was first proposed by American engineer Shannon in 1948 and can represent the information contained in the system. If all the possible grayscale information of the image is averaged, the information entropy is obtained. The so-called entropy refers to the average information, it is usually represented by H. Shannon's information theory proves that information entropy is the theoretical limit of undistorted coding, and the undistorted coding method below this limit does not exist, which is the theoretical basis of entropy coding. Now, information entropy has been introduced into image processing technology.

$$\mathrm{H}\ (\mathrm{x}) = \mathrm{E}\ [I(xi)] = E\ [\log(2, 1/p\ (xi))] = -\sum p\ (xi) \log(2, p\ (xi)) \quad (i = 1, 2, \ldots\ldots n) \tag{5}$$

In formula (5), H is in bits/characters, (xi) represents the random variable, and corresponding to it is the set of all possible outputs, defined as the symbol set, and the output of the random variable is represented by x. P(x) represents the output probability function. The information entropy is proportional to the uncertainty of the variable. Information entropy can directly show the amount of information contained in an image. If the value of information entropy H is smaller, it means that the system is more orderly and the image quality is higher. In this paper, the information entropy of the two methods at different sampling times is evaluated and analyzed.

As can be seen from the graph and table: (1) Green represents the information entropy change curve under the traditional ghost imaging method, and blue represents the information entropy change curve under the ghost imaging algorithm based on channel coding. (2) With the increase of sampling frequency, information entropy H value is on the decline, such as we can see from the blue curve, when the sampling frequency is 896, H value is 03989, and when the sampling frequency is 4096, H value is 0.2334. These directions as the sampling frequency, the greater the H value is smaller, on behalf of the system is more orderly and image quality is higher. (3) On the whole, the effect image information entropy H of ghost imaging algorithm based on channel coding is smaller than the traditional ghost imaging method, and with the increasing the number of sampling, the gap between the two is more and more big, when the sampling frequency is 4096, the effect image information entropy H of the ghost imaging algorithm based on channel coding is 0.2334, while the effect image information entropy H of the traditional ghost imaging method is 0.3433. In other words, the former system is orderly and have higher image quality. These experimental results show that the system of the scheme is more orderly and the image of the effect has better quality, which proves that the scheme is more effective in reliability.

5.2.4 Robustness: Noise attack is inevitable in the process of information transmission, and it will affect the quality of object imaging and destroy the image information transmission. Here, Salt-pepper noise and Speckle noise were selected to attack. Salt-pepper noise were 0.01, 0.02 and 0.04 respectively. Speckle noise were 0.1, 0.2 and 0.4 respectively. And the robustness of the scheme is evaluated by means of objective evaluation index Mean Square Error (MSE) and Peak Signal-to-Noise noise ratio (PSNR). For images of M $\times$ N size, the mathematical expression is as follows:

$$MSE = \frac{\sum_{i=1}^{M}\sum_{j=1}^{N}\left(V_{i,\,j} - V'_{i,\,j}\right)^2}{M \times N} \tag{5}$$

$$PSNR = 10\lg\frac{V_{\max}^2}{MSE} \tag{6}$$

$V_{i,\,j}$ and $V'_{i,\,j}$ denote the values of the pixels corresponding to the original image and the effect image respectively. $V_{\max}$ denotes the value of the largest pixel of the image. The higher the PSNR value, the higher the quality of the restored image.

As can be seen from the graph: (1) Red represents noise attack of 0.01, green represents noise attack of 0.02, and blue represents noise attack of 0.04. (2) Under the condition of noise attack of 0.04, when the sampling time is 96, the PSNR value is 15.3464; when the sampling time is 2496, the PSNR value is 16.9328; when the sampling time is 4096, the PSNR value is 18.7836. That is, with the increase of sampling times, PSNR value keeps increasing, and the quality of reconstructed images becomes higher and higher. (3) When the sampling time is 4096, noise attack corresponding PSNR value of 24.4627 to 0.01, noise attack corresponding PSNR value of 22.8112 to 0.02, because the quality of the reconstructed image is proportional to the PSNR, this experimental results show that the reconstructed images obtained by this scheme can still have good quality under salt-pepper noise attack.

As can be seen from the graph: (1) Red represents noise attack of 0.1, green represents noise attack of 0.2, and blue represents noise attack of 0.4. (2) Under the condition of noise attack of 0.4, when the sampling time is 96, the PSNR value is 20.4535; when the sampling time is 2496, the PSNR value is 23.4101; when the sampling time is 4096, the PSNR value is 27.4801. (3) When the sampling time is 4096, noise attack corresponding PSNR value of 33.7466 to 0.1, noise attack corresponding PSNR value of 30.7038 to 0.2. This experimental results show that the reconstructed images obtained by this scheme can still have good quality under speckle noise attack, which proves that the proposed scheme is effective in terms of robustness.

6. Conclusion

This paper proposes the algorithm of channel coding ghost imaging and studies its signal transmission mechanism, which solves the problems such as the lack of feasibility of the current imaging algorithm, the low degree of detail reduction of complex objects, the long imaging time, and so on. This algorithm breaks through the limitation of traditional ghost imaging. In the process of channel coding combined with ghost imaging, which can achieve high resolution ultra-fast signal transmission, it can greatly reduce the error rate, decrease the time of image reconstruction and improve the running efficiency. Because of the principle of correlating imaging zero memory retrieval and the characteristic of “non-locality”, which is not found in classical imaging. At the same time, the characteristics of the LDPC linear block code are used to reduce the storage space, thereby further improving the transmission efficiency and achieving accurate image encoding and transmission. And it has a strong immune effect on environmental noise, and can achieve better signal-to-noise ratio and contrast. On the basis of channel coding, ghost imaging has a strong anti-jamming ability compared with traditional imaging, so it can improve the system’s error-correcting ability and transmission signal reliability, and reducing the bit error rate. This secure and reliable communication method based on LDPC code is a type of anti-jamming and anti-interception communication mode in coding domain, it ensures the reliability of the system through the random change of the channel coding matrix, enhances the difficulty of decoding by the attackers, and greatly improves the security of the communication system based on LDPC code. Combined with the algorithm of ghost imaging, high quality reconstruction on large scale images can be realized, and the security performance of traditional imaging can be overcome. The reasonable setting of chaotic light source can effectively improve the transmission security and increase the difficulty of deciphers. Therefore, this method has a good application prospect.

Reference

[1] A. Fukata, “Coding device, imaging device, coding transmission system, and coding method,” 2017.

[2] J. H. Shapiro and R. W. Boyd, “The physics of ghost imaging,” *Quantum Inf. Process.*, vol. 11, pp. 949–993, 2012.

[3] N. D. Hardy and J. H. Shapiro, “Computational ghost imaging versus imaging laser radar for three-dimensional imaging,” *Phys. Rev. A*, vol. A87, 2013, Art. no. 023820.

[4] H. Liu and J. Xiong, “Properties of high-order ghost imaging with natural light,” *J. Opt. Soc. Amer.*, vol. A 30, pp. 956–961, 2013.

[5] H. Li, J. Shi, and G. Zeng, “Ghost imaging with nonuniform thermal light fields,” *J. Opt. Soc. Amer.*, vol. A30, pp. 1854–1861, 2013.

[6] D. B. Phillips *et al.*, “Non-diffractive computational ghost imaging,” *Opt. Exp.*, vol. 24, no. 13, pp. 14172–14182, 2016.
[7] B. Sun, S. S. Welsh, M. P. Edgar, J. H. Shapiro, and M. J. Padgett, “Normalized ghost imaging,” *Opt. Exp.*, vol. 20, pp. 16892–16901, 2012.
[8] Z. Liu, S. Tan, and J. Wu, “Spectral camera based on ghost imaging via sparsity constraints,” *Sci. Rep.*, vol. 6, 2016, Art. no. 25718.
[9] J Chen, W Gong, and S Han, “Sub-rayleigh ghost imaging via sparsity constraints based on a digital micro-mirror device,” *Phys. Lett.*, vol. A 377, pp. 1844–1847, 2013.
[10] V. Katkovnik and J. Astola, “Compressive sensing computational ghost imaging,” *J. Opt. Soc. Amer.*, vol. A29, pp. 1556–1567, 2012.
[11] A. Pompeii and F. Selleri, “Possible epr experiment with neutral pseu do-scalar meson-antimeson correlated pairs,” *Frontiers Part Phys.*, 2017.
[12] J. H. Shapiro, “Computational ghost imaging,” *Phys Rev.*, vol. A78, pp. 1–2, 2008.
[13] Y. J. Zhong *et al.*, “Multiple speckle patterns differential compressive ghost imaging,” *Acta Physica Sinica*, vol. 64, no. 1, pp. 88–94, 2015.
[14] I. B. Djordjevic, “Channel coding for optical transmission systems,” in *Proc. Opto-Electron. Commun. Conf.*, 2017, pp. 1–2.
[15] G. He *et al.*, “Research on secure communication based on LDPC code,” in *Proc. Int. Conf. Wireless Commun. Sensor Netw.*, 2016. pp. 105–110.
[16] C. Zhou, Q. Sun, and J. Liu, “Method to generate diagonalizable LDPC measurement matrix based on compressive sensing,” *Comput. Sci.*, vol. 44, pp. 279–282, 2017.
[17] M. Ren, “Simulation research on optimization of compression image transmission extraction and reconstruction,” *Comput Simul.*, vol. 7, pp. 316–319, 2017.
[18] S. H. Bae, J. Kim, and M. Kim, “HEVC-based perceptually adaptive video coding using a DCT-based local distortion detection probability model,” *IEEE Trans. Image Process.*, vol. 25, no. 7, 2016, pp. 3343–3357.
[19] T. Mao, Q. Chen, and W. He, “Optical communication in turbid and turbulent atmosphere,” *Acta Phys. Sin.*, vol. 65, 2016, Art. no. 084207.
[20] M. Morii, H. Tamiya, and M. Hirotomo, “Error correction capability of irregular LDPC codes under the Gallager a algorithm,” in *Proc. IEEE Int. Symp. Inf. Theory Appl.* 2017.